NASA TN D-726

Copy 2

TECHNICAL NOTE

D-726

AN INVESTIGATION OF HIGH-VELOCITY IMPACT CRATERING INTO NONMETALLIC TARGETS AND CORRELATION OF PENETRATION DATA FOR METALLIC AND NONMETALLIC TARGETS

By William H. Kinard and Rufus D. Collins, Jr.

Langley Research Center
Langley Field, Va.

NATIONAL AERONAUTICS AND SPACE ADMINISTRATION

WASHINGTON

February 1961

NATIONAL AERONAUTICS AND SPACE ADMINISTRATION

TECHNICAL NOTE D-726

AN INVESTIGATION OF HIGH-VELOCITY IMPACT CRATERING INTO NONMETALLIC TARGETS AND CORRELATION OF PENETRATION DATA FOR METALLIC AND NONMETALLIC TARGETS

By William H. Kinard and Rufus D. Collins, Jr.

SUMMARY

Experimental results have been obtained on the cratering of metals and nonmetals at velocities varying from 500 feet per second to 20,000 feet per second with various combinations of metallic and nonmetallic targets and projectiles. Materials investigated include nylon, graphite, laminated phenolic resin, and aluminum. From a study of nonmetallic targets after impact, it is indicated that the craters were formed by the crushing of and displacement of the target material. An equation for the relationship between penetration and momentum per unit area has been modified to predict the penetration of target materials tested within the range of this investigation.

INTRODUCTION

The advent of space travel has brought about a mounting interest in the cratering and damage resulting from the impact of very high-velocity particles. Space vehicles can be subjected to uninterrupted bombardment of meteoroids at impact velocities as great as 240,000 feet per second. These space vehicles must be designed to withstand catastrophic impacts before man can safely venture into space for extended periods of time. Interest in impact cratering at lower velocities is confined to the development of weapon systems which depend upon projectile impacts with a target at impact velocities below 20,000 feet per second.

At the present, laboratory techniques do not permit the achievement of impact velocities approaching those of the meteorites; however, impact velocities common to most weapon systems are obtainable. Previous investigations have dealt primarily with the impact of projectiles into metal targets. Impact data in metal targets are included in references 1 and 2.

Lightweight nonmetal materials such as plastics offer a solution to many structural and environmental requirements of space traveling vehicles. It has been the aim of this investigation to study the cratering resulting from the impact of various metallic and nonmetallic combinations of projectiles and targets. The impact velocities achieved in this investigation are in the range of 500 to 20,000 feet per second, but, unfortunately, are far below the velocities of meteorites in space. With the lack of more realistic data on meteorites, the results of this investigation may give some indication of the damage to expect.

SYMBOLS

b	momentum per unit area necessary to produce permanent deformation, lb-sec/sq in.
d	diameter of projectile, in.
E	modulus of elasticity of target material, lb/sq in.
K_p	projectile deformation factor
K_t	reciprocal of the target resistance factor
l	maximum length of projectile normal to the point of impact, in.
P	penetration, in.
V	projectile velocity, fps
ρ	mass density of projectile, slugs/cu in.

Subscripts:

p	projectile
t	target

APPARATUS AND TEST TECHNIQUE

Description of Projectiles and Targets

The projectile materials used in this investigation consisted of commercially pure copper, 2024-T4 aluminum, commercially pure lead,

cold-rolled steel having a carbon range from 0.12 to 0.30 and a manganese range from 0.30 to 0.60, and molded thermoplastic nylon. The projectiles consisted of various size spheres with diameters ranging from 0.0390 inch to 0.220 inch, right circular cylinders having diameters of 0.220 inch with a length-to-diameter ratio of 1, and cone cylinders having diameters of 0.220 inch with a length-to-diameter ratio of 0.910.

Target materials used in this investigation are listed in the following table:

Material	Designation	Modulus of elasticity, E, lb/sq in.
Bakelite	Type 2, grade C.E. meeting Federal specifications L-L-31; 4 to 6 inches in diameter, paper laminations	9×10^5 lengthwise of the laminations; 8×10^5 crosswise of the laminations
Graphite	AGX; 4- and 8-inch diameters	8×10^5
Nylon	Molded thermoplastic; 1- and 2-inch diameters	2×10^5
Aluminum	2024-T4; rods and plates of various sizes	1×10^7

Graphite targets were rods having diameters between 4 and 8 inches. The nylon targets were rods 1 inch and 2 inches in diameter. The aluminum targets were rods and plates of various sizes.

Accelerators

Three guns were used in the course of this investigation to accelerate the projectiles. A conventional 220-caliber Swift rifle was used to propel the projectiles to velocities of 6,000 feet per second through the atmosphere. A helium gun fired into a vacuum chamber was used to accelerate projectiles to velocities of 12,000 feet per second. A description and photograph of these two gun facilities are presented in reference 1.

Impact data of nylon projectiles and aluminum targets were obtained by using a double-gun facility such as described in reference 2.

Testing

The targets used in this investigation were positioned such that the projectiles impacted normal to the target surface. In each firing the projectile impact velocity was determined. The techniques used to measure the projectile velocities on each of the guns used are given in references 1 and 2 along with the gun descriptions. Basically, trigger signals that started and stopped an electronic time interval counter were obtained from two stations a known distance apart. Each signal was obtained as the projectile punctured a thin plastic film coated on both sides with a thin layer of aluminum to which a voltage potential was applied. The penetration of the projectile shorted the aluminum coatings and supplied the trigger pulses to start and stop the electronic counter at predetermined locations.

RESULTS AND DISCUSSION

The penetration data of this investigation have been presented in figures 1 to 6 and in table I. No attempt was made to present or correlate data related to crater diameters and volumes. Crater volumes in the nonmetal targets tested in this investigation were long slender cavities filled with crushed and pulverized material. Accurate measurements of crater diameters and volumes could not be obtained. The cratering observed in each of the target materials tested in this investigation are discussed in subsequent sections.

Laminated Phenolic Resin Targets

The craters observed in the laminated resin targets were quite different from those usually observed in metal targets after impact of high-velocity projectiles. High-velocity impacts in metal targets usually produce hemispherical cavities that appear to result from the plastic hydrodynamic behavior of the material during impact. Craters observed in the laminated targets of this investigation were relatively long and slender and had diameters slightly greater than the diameter of the impacting projectile. Cross sections of these craters show that the projectile had penetrated to a depth considerably below the bottom of the apparent crater and was completely surrounded by the target material.

A typical crater of this type is shown in figure 1(a). It can be seen that material behind the projectile and surrounding the crater has been crushed. It appears that the crater, during one stage of formation, was an open cavity with the material displaced compressively. As the pressures generated during impact were relieved, the crater or cavity

collapsed with much of its volume being filled with material crushed during the displacement and expansion.

This hypothesis is substantiated by a sequence of photographs, taken at a framing rate of 500,000 frames per second, showing the formation of similar craters in a Lucite target impacted by a spherical projectile. These photographs are presented in figure 2. The Lucite target was selected since it is transparent and the cratering could be observed. Polarized light and an analyzer were employed in taking the pictures so that target regions under stress would be visible. Shortly after impact, an elastic compression wave can be observed propagating from the point of impact in a hemispherical pattern. After the maximum penetration was obtained, material continued to be ejected from the crater. This is exactly as would be expected if the cavity were open and then had collapsed when the stresses of impact were relieved. This phenomenon has been reported previously in the collapsing of conical liners in studies of shaped explosive charges. This investigation is described in reference 3.

The collapsing of the crater is not visible in the photographs, because of the material in the vicinity of the crater being stressed to such a point as to rotate the plane of polarization of the light out of the transmission plane of the analyses; thus, this region of the target appears to be black.

Craters formed in the laminated targets did not exhibit the characteristic petals or lip surrounding the crater which is usually observed in metal targets. It appears that the material which would normally form the lip of a metal crater is spalled away from the bakelite targets. This is probably because of the low tensile strength properties possessed by laminated resin material. In some cases, broad areas of the target surface surrounding the craters have been damaged because the material has been spalled away.

Graphite Targets

The craters formed in graphite targets were found to be quite similar to those found in the laminated resin targets. Figure 1(b) illustrates a typical crater formed in a graphite target. It may be noted that there is no evidence of the graphite target material behaving plastically during the time of impact. It appears that the material was crushed under the impact load and the crater filled with the pulverized material, part of which was ejected from the crater. No lip or petals were formed around the crater but considerable surface material surrounding the cavity was spalled away. Damage and failure of the graphite target were not confined to the immediate target area alone.

Numerous cracks were observed which had propagated deep into the bulk of the target material.

Nylon Targets

The mechanics of cratering in nylon targets appeared to be very similar to those observed in the laminated resin and graphite targets. A typical nylon crater is shown in figure 1(c). The craters were deep slender cavities which appear to be typical of impact craters in plastic targets within the range of impact velocities obtainable in this investigation. Very little material was removed from the crater as illustrated in figure 1(c). Cracks were formed in the nylon material at low velocities. At the highest velocity impacts obtained in this investigation, large quantities of the surface material were broken from the target. The breakup was obviously the result of the reflection of strong compression waves generated at impact from the face surfaces of the relatively small diameter targets. Data analysis indicates that this fracturing and breakup had little effect on the actual penetration depths achieved.

Aluminum Targets

This investigation has dealt primarily with the cratering mechanics of nonmetallic targets. In contrast to metal projectiles impacting nonmetallic targets, this series consists of nylon projectiles impacting aluminum targets at impact velocities up to 20,000 feet per second. The craters formed in the aluminum targets were mostly hemispherical cavities. Aluminum targets were used as a comparison and check of the nonmetal-target data analysis.

CORRELATION OF PENETRATION DATA

In reference 1 it has been established that the penetration of aluminum, copper, lead, and steel projectiles impacting into aluminum, copper, and steel targets can be correlated as a linear function of the maximum momentum per unit area possessed by the projectile at impact. The maximum momentum per unit area is defined as $\rho_p V l$. The equation found to describe the data was of the form

$$P = K_p K_t \left(\rho_p V l - b\right) \qquad (1)$$

The values of K_p, K_t, and b were obtained from data at impact velocities up to 13,000 feet per second. It was observed in reference 1 that the value of K_p varied as an inverse function of the projectile density. The value of K_t varied inversely with the elastic modulus of the target material. It therefore appears that equation (1) can be simplified and the constants K_p and K_t expressed as functions of the projectile density and target modulus of elasticity, respectively.

The penetration data obtained in this investigation were plotted as a function of the maximum momentum per unit area possessed by the impacting projectile and are shown in figures 1 to 6. The value of K_p for nylon projectiles and the values of K_t for the laminated resin, graphite, and nylon targets were then determined by the method described in reference 1.

In figure 7 the K_p values from reference 1 and the value obtained in this investigation for nylon projectiles have been plotted against the corresponding projectile density. The expression

$$K_p = 0.309(\rho_p)^{-0.278} \tag{2}$$

closely predicts the experimentally determined values of K_p.

In figure 8 the K_t values from reference 1 and the K_t values established in this investigation for laminated resin, graphite, and nylon targets have been plotted as a function of the target modulus of elasticity. It can be observed from figure 8 that the equation

$$K_t = \left(\frac{175{,}000}{E + 2{,}800{,}000}\right)^{0.78} \tag{3}$$

predicts the experimentally determined values of K_t within engineering accuracy.

Substituting equations (2) and (3) for the value of K_p and K_t into equation (1) and simplifying yields

$$P = \frac{3797(\rho_p V l - b)}{(\rho_p)^{0.278}(E + 2.8 \times 10^6)^{0.78}} \tag{4}$$

which adequately predicts the penetration results in reference 1 and this investigation, the units of the constant 3797 being such as to make the equation dimensionally correct. The lines of equation (4) are shown in figures 1 to 6. It is observed that the penetration data of this investigation are predicted within an order of magnitude accuracy. The value of b in equation (4) was assumed to be zero for the laminated resin, graphite, and nylon targets since these materials have low modulus of elasticities and offer little resistance to initial penetration. The units of the constant 3797 are such as to make the penetration units inches.

CONCLUDING REMARKS

The data obtained in this investigation have indicated that the same projectile and target properties govern penetration in both metallic and nonmetallic target materials throughout a velocity range from 500 feet per second to 20,000 feet per second. The physical appearance of craters was found to be very different in metallic and nonmetallic target materials. The craters formed in metal targets are open hemispherical cavities whereas craters in nonmetallic targets in the velocity range of this investigation are slender partially filled cavities.

An equation for the relationship between penetration and momentum per unit area, obtained in this investigation, has been shown to predict the penetration of impacting particles having a density range between 0.048 and 0.42 pound per cubic inch into targets of metals and nonmetals having an elastic modulus range between 200,000 lb/sq in. and 30,000,000 lb/sq in. This equation should therefore predict the penetration of particles impacting most materials of interest within the velocity range of the data from which the equation was established.

Langley Research Center,
National Aeronautics and Space Administration,
Langley Field, Va., December 21, 1960.

REFERENCES

1. Collins, Rufus D., Jr., and Kinard, William H.: The Dependency of Penetration on the Momentum Per Unit Area of the Impacting Projectile and the Resistance on Materials to Penetration. NASA TN D-238, 1960.

2. Kinard, William H., and Collins, Rufus D., Jr.: A Technique for Obtaining Hypervelocity Impact Data by Using the Relative Velocities of Two Projectiles. NASA TN D-724, 1961.

3. Pugh, Emerson M., Eichelberger, R. J., and Rostoker, Norman: Theory of Jet Formation by Charges With Lined Conical Cavities. Jour. Appl. Phys., vol. 23, no. 5, May 1952, pp. 532-536.

TABLE I.- HIGH-VELOCITY-IMPACT DATA

Projectile	Projectile material	Target material	Velocity, fps	Penetration, in.
0.039-inch-diameter sphere				
1	Steel	Nylon	3,564	0.090
2	Steel	Nylon	5,049	.200
3	Steel	Nylon	6,831	.377
4	Steel	Nylon	8,019	.480
5	Steel	Nylon	9,504	.552
6	Steel	Nylon	9,652	.570
0.062-inch-diameter sphere				
*7	Aluminum	Laminated resin	1,554	0.025
*8	Aluminum	Laminated resin	2,021	.065
*9	Aluminum	Laminated resin	2,694	.048
*10	Aluminum	Laminated resin	4,093	.060
*11	Aluminum	Laminated resin	5,181	.078
*12	Aluminum	Laminated resin	5,803	.078
*13	Aluminum	Laminated resin	6,788	.100
**14	Steel	Laminated resin	2,015	.030
**15	Steel	Laminated resin	2,292	.025
**16	Steel	Laminated resin	3,438	.048
**17	Steel	Laminated resin	4,621	.055
**18	Steel	Laminated resin	4,805	.038
**19	Steel	Laminated resin	6,007	.070
**20	Steel	Laminated resin	6,617	.145
**21	Steel	Laminated resin	6,875	.125
22	Aluminum	Graphite	1,298	.040
23	Aluminum	Graphite	1,558	.050
24	Aluminum	Graphite	2,077	.090
25	Aluminum	Graphite	2,597	.110
26	Aluminum	Graphite	2,908	.150
27	Aluminum	Graphite	3,480	.165
28	Aluminum	Graphite	4,518	.170
29	Aluminum	Graphite	5,193	.210
30	Aluminum	Graphite	5,713	.230
31	Aluminum	Graphite	6,232	.250
32	Aluminum	Graphite	8,569	.270
33	Copper	Graphite	2,565	.360
34	Copper	Graphite	4,328	.390
35	Copper	Graphite	5,579	.415
36	Copper	Graphite	6,989	.500
37	Steel	Graphite	924	.035
38	Steel	Graphite	1,146	.050
39	Steel	Graphite	1,442	.060
40	Steel	Graphite	2,384	.075
41	Steel	Graphite	2,754	.085

*Impacts parallel to target laminations.
**Impacts perpendicular to target laminations.

TABLE I.- HIGH-VELOCITY-IMPACT DATA - Continued

Projectile	Projectile material	Target material	Velocity, fps	Penetration, in.
0.062-inch-diameter sphere				
42	Steel	Graphite	3,696	0.100
43	Steel	Graphite	4,621	.130
44	Steel	Graphite	5,563	.159
45	Steel	Graphite	6,099	.177
46	Steel	Graphite	6,654	.200
47	Steel	Graphite	7,190	.250
48	Steel	Nylon	1,663	.062
49	Steel	Nylon	2,310	.120
50	Steel	Nylon	3,419	.278
51	Steel	Nylon	3,955	.370
52	Steel	Nylon	4,436	.450
53	Steel	Nylon	4,990	.520
54	Steel	Nylon	5,582	.600
55	Steel	Nylon	6,136	.635
56	Steel	Nylon	6,968	.670
57	Steel	Nylon	7,374	.698
58	Steel	Nylon	7,578	.690
59	Steel	Nylon	7,578	.680
60	Steel	Nylon	10,849	.868
61	Steel	Nylon	11,089	.895
0.090-inch-diameter sphere				
62	Lead	Graphite	1,002	0.160
63	Lead	Graphite	1,222	.210
64	Lead	Graphite	1,438	.220
65	Lead	Graphite	2,008	.410
66	Lead	Graphite	2,050	.300
67	Lead	Graphite	2,441	.490
68	Lead	Graphite	3,140	.600
69	Lead	Graphite	4,240	.685
0.125-inch-diameter sphere				
70	Steel	Graphite	1,238	0.110
71	Steel	Graphite	1,513	.132
72	Steel	Graphite	1,980	.170
73	Steel	Graphite	2,274	.190
74	Steel	Graphite	2,952	.245

TABLE I.- HIGH-VELOCITY-IMPACT DATA - Continued

Projectile	Projectile material	Target material	Velocity, fps	Penetration, in.
0.125-inch-diameter sphere				
75	Steel	Graphite	3,594	0.270
76	Steel	Graphite	4,584	.300
77	Steel	Graphite	5,116	.327
78	Steel	Graphite	5,748	.360
79	Steel	Graphite	6,527	.381
80	Steel	Graphite	6,802	.400
0.22-inch-diameter sphere				
*81	Aluminum	Laminated resin	571	0.065
*82	Aluminum	Laminated resin	893	.020
*83	Aluminum	Laminated resin	1,772	.122
*84	Aluminum	Laminated resin	2,782	.224
*85	Aluminum	Laminated resin	3,909	.325
*86	Aluminum	Laminated resin	4,407	.362
*87	Aluminum	Laminated resin	5,725	.370
*88	Aluminum	Laminated resin	6,135	.415
*89	Aluminum	Laminated resin	6,750	.457
*90	Copper	Laminated resin	1,165	.222
*91	Copper	Laminated resin	2,498	.660
*92	Copper	Laminated resin	2,882	.970
*93	Copper	Laminated resin	2,959	1.218
*94	Copper	Laminated resin	4,039	1.445
*95	Copper	Laminated resin	4,879	1.704
*96	Copper	Laminated resin	4,969	1.340
**97	Copper	Laminated resin	1,446	.175
**98	Copper	Laminated resin	1,762	.235
**99	Copper	Laminated resin	2,024	.320
**100	Copper	Laminated resin	2,259	.405
**101	Copper	Laminated resin	3,659	.880
**102	Copper	Laminated resin	4,418	.760
**103	Copper	Laminated resin	4,558	.925
**104	Copper	Laminated resin	4,769	.900
**105	Copper	Laminated resin	5,285	.940
*106	Lead	Laminated resin	1,103	.325
*107	Lead	Laminated resin	1,292	.330
*108	Lead	Laminated resin	1,364	.455
*109	Lead	Laminated resin	1,435	.421
*110	Lead	Laminated resin	2,006	.420
*111	Lead	Laminated resin	2,745	.612
*112	Lead	Laminated resin	3,638	.821
*113	Lead	Laminated resin	3,912	.642

*Impacts parallel to target laminations.
**Impacts perpendicular to target laminations.

TABLE I.- HIGH-VELOCITY-IMPACT DATA - Continued

Projectile	Projectile material	Target material	Velocity, fps	Penetration, in.
0.22-inch-diameter sphere				
*114	Lead	Laminated resin	3,916	0.900
*115	Steel	Laminated resin	1,146	.140
*116	Steel	Laminated resin	1,615	.245
*117	Steel	Laminated resin	1,636	.310
*118	Steel	Laminated resin	1,703	.490
*119	Steel	Laminated resin	1,823	.368
*120	Steel	Laminated resin	3,115	.690
*121	Steel	Laminated resin	3,886	1.00
*122	Steel	Laminated resin	4,506	1.325
*123	Steel	Laminated resin	5,078	1.625
*124	Steel	Laminated resin	5,532	1.66
*125	Steel	Laminated resin	5,912	1.36
**126	Steel	Laminated resin	1,119	.187
**127	Steel	Laminated resin	1,832	.290
**128	Steel	Laminated resin	2,330	.390
**129	Steel	Laminated resin	2,872	.590
**130	Steel	Laminated resin	3,788	.930
**131	Steel	Laminated resin	4,420	1.190
**132	Steel	Laminated resin	5,180	1.290
**133	Steel	Laminated resin	5,462	1.315
**134	Steel	Laminated resin	5,840	1.233
135	Aluminum	Graphite	3,366	.414
136	Aluminum	Graphite	4,610	.660
137	Aluminum	Graphite	6,147	.653
138	Aluminum	Graphite	6,732	.650
0.22-inch-diameter cylinder; $l/d = 1$				
*139	Aluminum	Laminated resin	2,035	0.355
*140	Aluminum	Laminated resin	2,313	.363
*141	Aluminum	Laminated resin	2,635	.335
*142	Aluminum	Laminated resin	3,089	.155
*143	Aluminum	Laminated resin	4,363	.400
*144	Aluminum	Laminated resin	4,392	.240
*145	Aluminum	Laminated resin	5,417	.350
*146	Aluminum	Laminated resin	6,325	.320
*147	Aluminum	Laminated resin	7,057	.485
*148	Copper	Laminated resin	1,287	.360
*149	Copper	Laminated resin	1,581	.422
*150	Copper	Laminated resin	1,834	.283
*151	Copper	Laminated resin	2,083	.400
*152	Copper	Laminated resin	2,968	.685

*Impacts parallel to target laminations.
**Impacts perpendicular to target laminations.

TABLE I.- HIGH-VELOCITY-IMPACT DATA - Continued

Projectile	Projectile material	Target material	Velocity, fps	Penetration, in.
0.22-inch-diameter cylinder; $l/d = 1$				
*153	Copper	Laminated resin	3,569	0.815
*154	Copper	Laminated resin	4,156	.920
*155	Copper	Laminated resin	4,599	1.057
*156	Copper	Laminated resin	5,285	1.120
**157	Copper	Laminated resin	1,220	.140
**158	Copper	Laminated resin	1,581	.185
**159	Copper	Laminated resin	1,897	.230
**160	Copper	Laminated resin	2,259	.280
**161	Copper	Laminated resin	2,973	.522
**162	Copper	Laminated resin	3,659	.760
**163	Copper	Laminated resin	4,066	.875
**164	Copper	Laminated resin	5,051	1.013
**165	Copper	Laminated resin	5,421	1.050
*166	Lead	Laminated resin	1,017	.245
*167	Lead	Laminated resin	1,553	.280
*168	Lead	Laminated resin	1,692	.596
*169	Lead	Laminated resin	2,006	.460
*170	Lead	Laminated resin	3,070	.620
*171	Lead	Laminated resin	3,569	.810
*172	Lead	Laminated resin	4,105	.943
*173	Steel	Laminated resin	1,292	.190
*174	Steel	Laminated resin	1,620	.242
*175	Steel	Laminated resin	1,927	.428
*176	Steel	Laminated resin	2,844	.530
*177	Steel	Laminated resin	3,750	.940
*178	Steel	Laminated resin	4,167	.970
*179	Steel	Laminated resin	4,828	1.110
*180	Steel	Laminated resin	5,308	1.222
*181	Steel	Laminated resin	5,453	1.25
**182	Steel	Laminated resin	1,172	.150
**183	Steel	Laminated resin	1,483	.195
**184	Steel	Laminated resin	2,188	.332
**185	Steel	Laminated resin	2,998	.448
**186	Steel	Laminated resin	3,651	.637
**187	Steel	Laminated resin	4,210	.770
**188	Steel	Laminated resin	4,675	.870
**189	Steel	Laminated resin	5,093	.903
**190	Steel	Laminated resin	5,470	.970
191	Aluminum	Graphite	3,073	.410
192	Aluminum	Graphite	4,171	.560
193	Aluminum	Graphite	5,869	.630
194	Aluminum	Graphite	6,879	.740

*Impacts parallel to target laminations.
**Impacts perpendicular to target laminations.

TABLE I.- HIGH-VELOCITY-IMPACT DATA - Concluded

Projectile	Projectile material	Target material	Velocity, fps	Penetration, in.
0.22-inch-diameter cone cylinder; l/d = 0.910				
195	Nylon	Aluminum	1,845	0
196	Nylon	Aluminum	4,190	.01
197	Nylon	Aluminum	5,290	.011
198	Nylon	Aluminum	5,440	.019
199	Nylon	Aluminum	6,780	.067
200	Nylon	Aluminum	7,180	.067
201	Nylon	Aluminum	10,510	.098
202	Nylon	Aluminum	12,050	.132
203	Nylon	Aluminum	13,760	.185
204	Nylon	Aluminum	17,050	.240
205	Nylon	Aluminum	19,950	.300

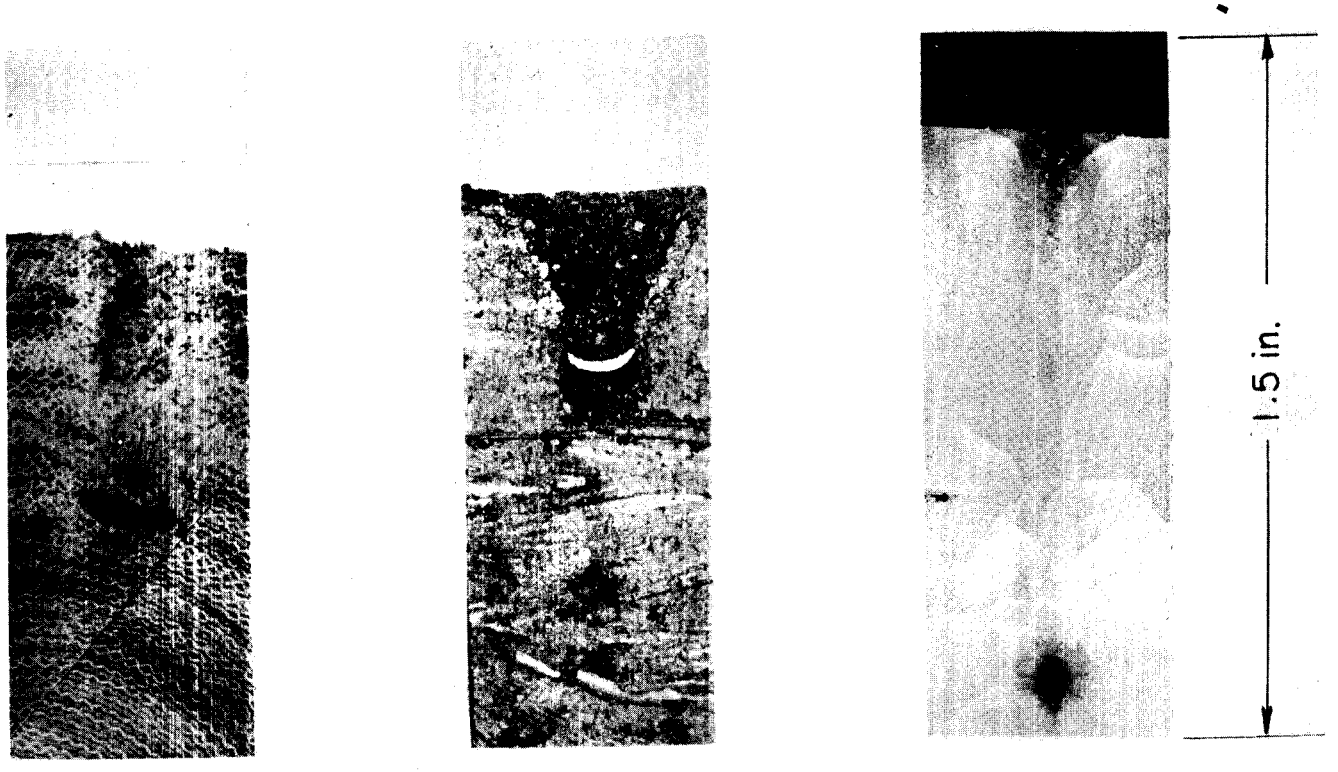

L-60-8321

(a) Laminated phenolic resin target.

(b) Graphite target.

(c) Nylon target.

Figure 1.- Typical craters formed in the nonmetal targets used in this investigation.

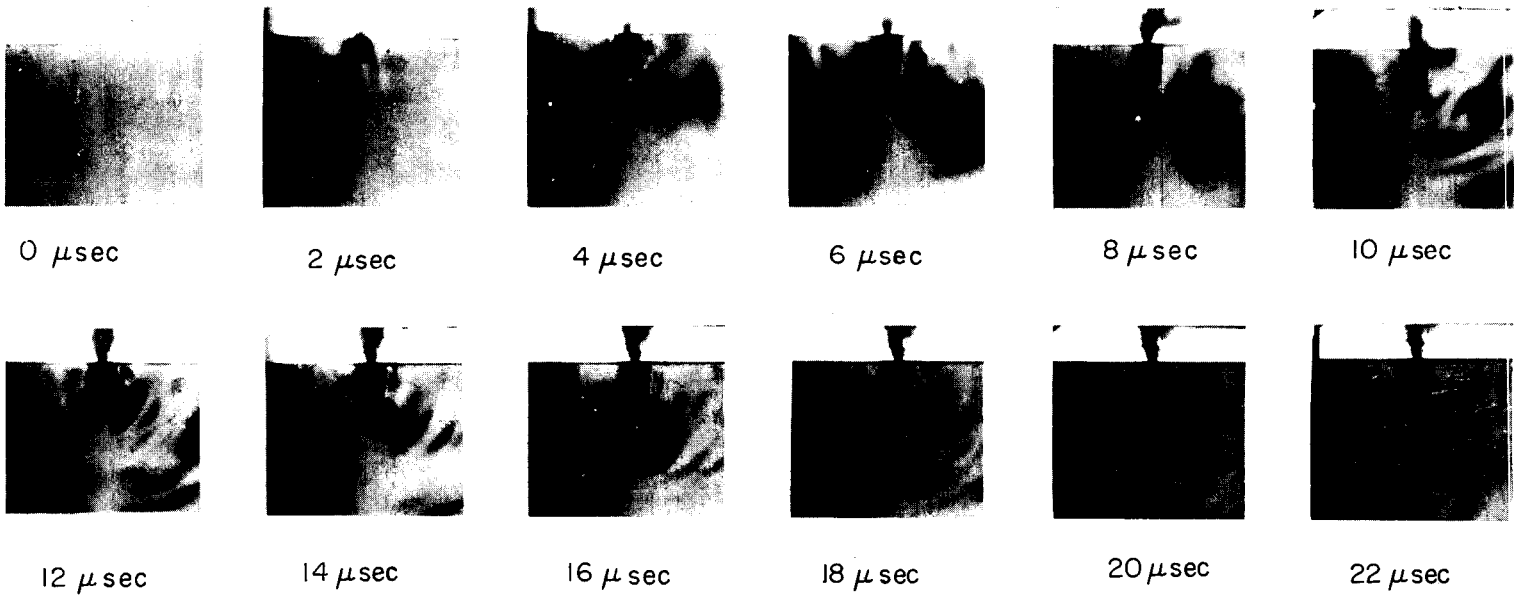

L-60-8322

Figure 2.- Photostress pictures of a 1/16-inch-diameter projectile impacting a Lucite target.

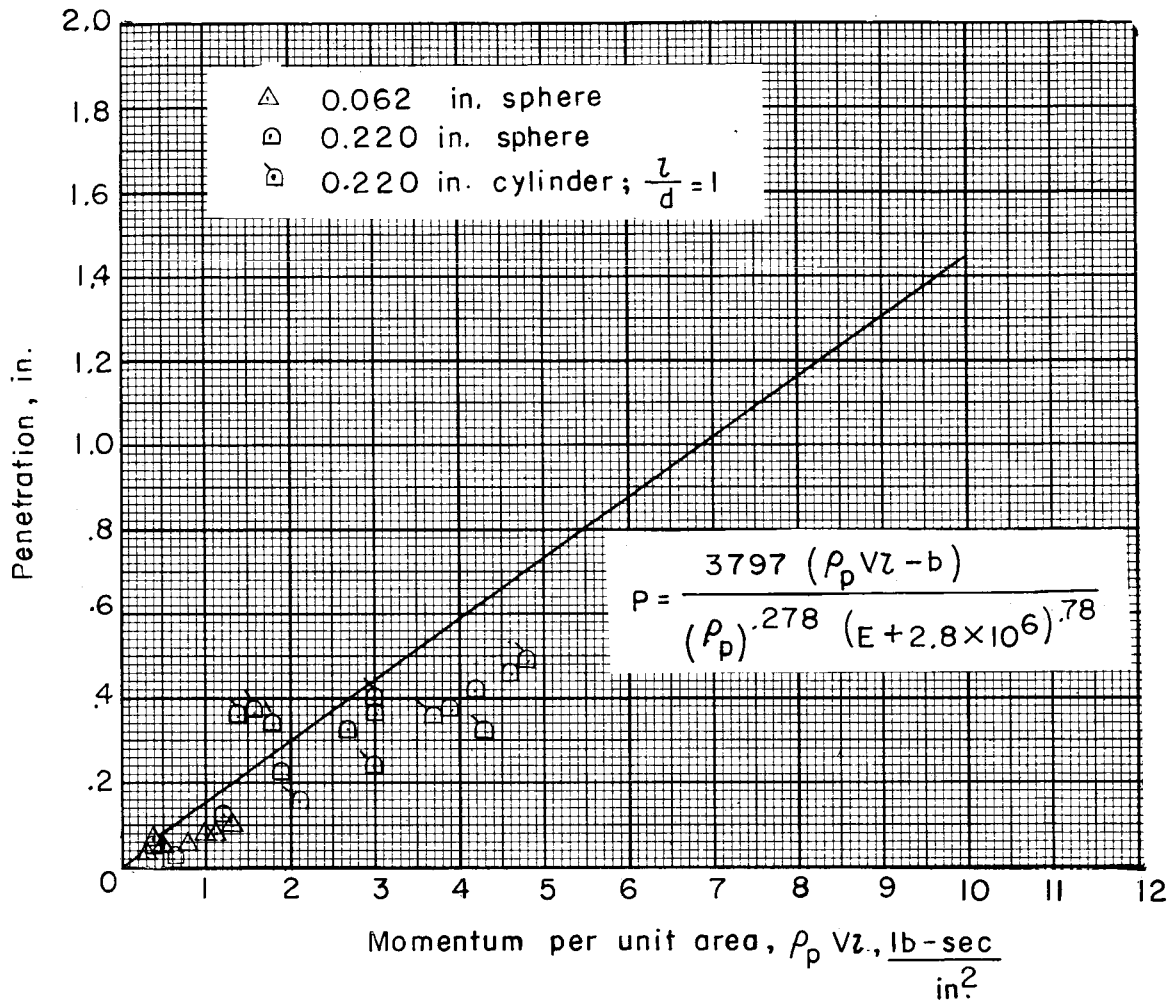

(a) Aluminum projectiles with impact direction parallel to target laminations.

Figure 3.- Data of impacts in laminated phenolic resin targets.

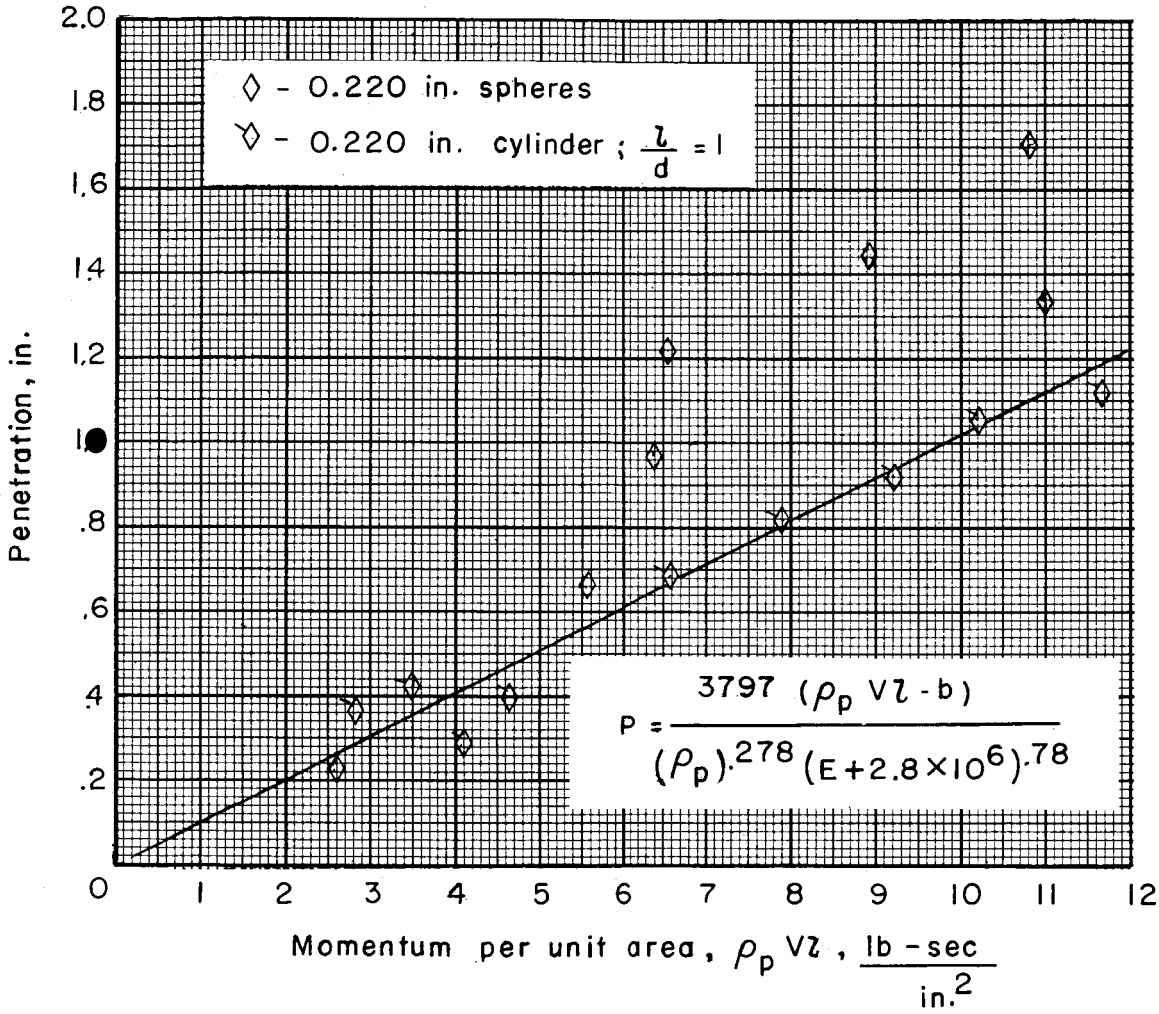

(b) Copper projectiles with impact direction parallel to target laminations.

Figure 3.- Continued.

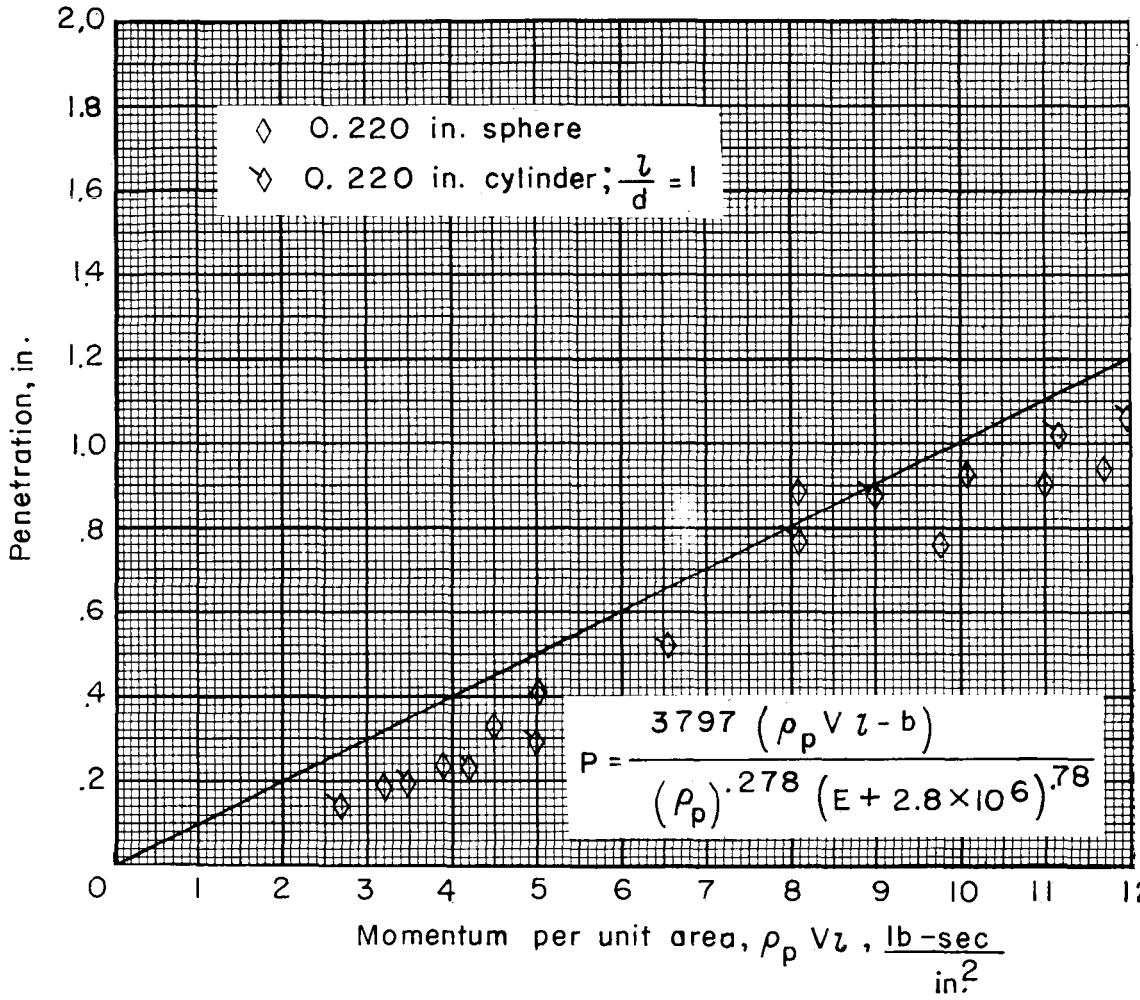

(c) Copper projectiles with impact direction perpendicular to target laminations.

Figure 3.- Continued.

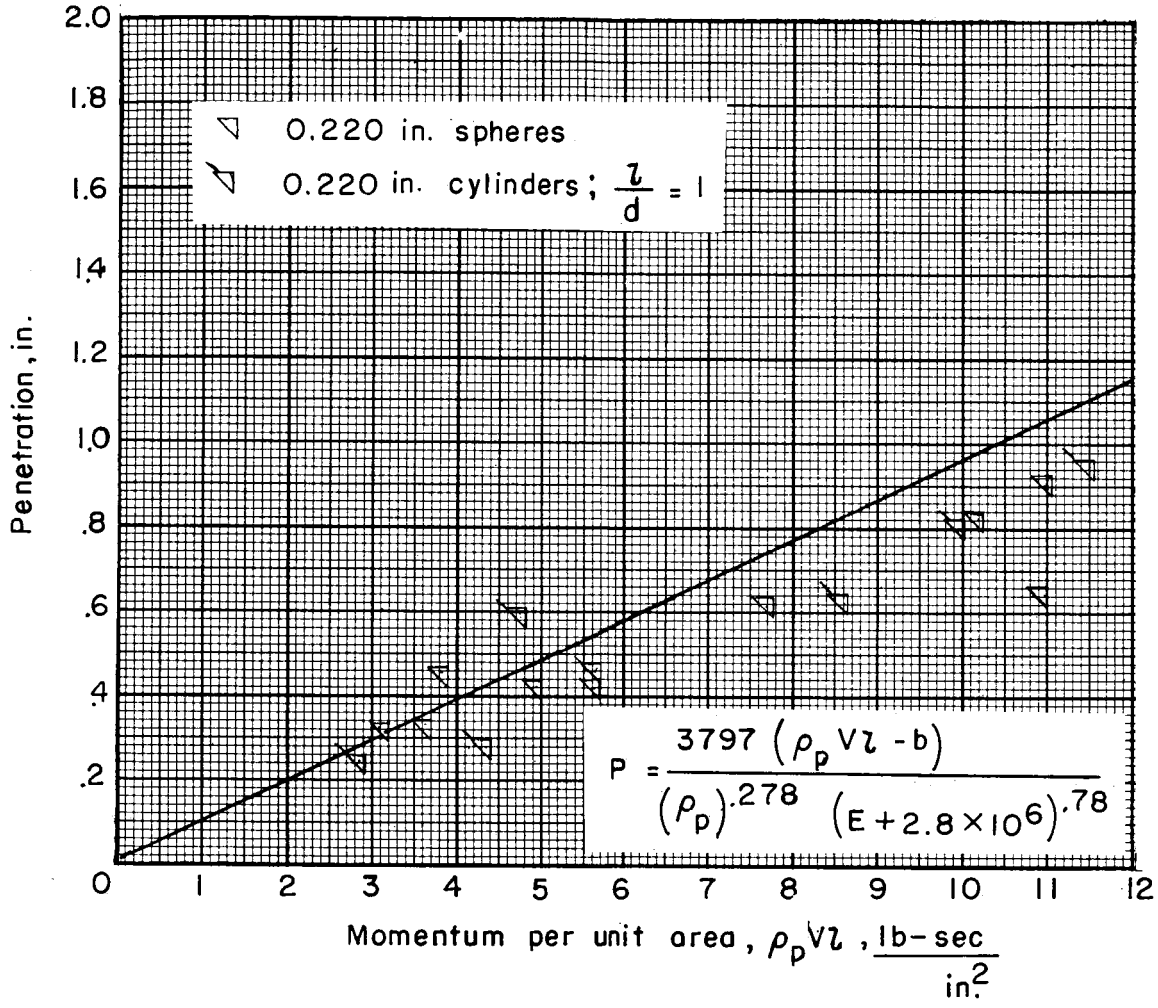

(d) Lead projectiles with impact direction parallel to target laminations.

Figure 3.- Continued.

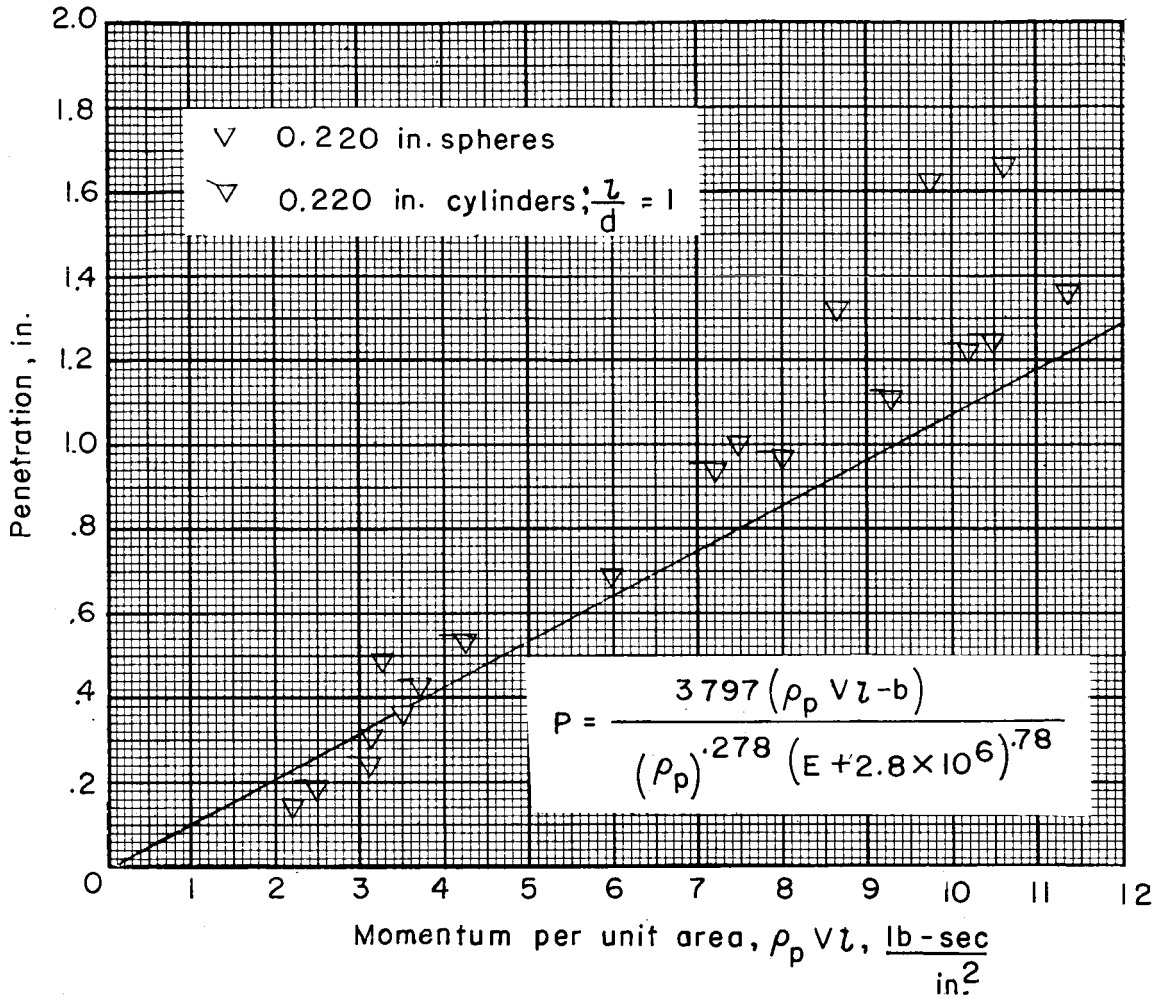

(e) Steel projectiles with impact direction parallel to target laminations.

Figure 3.- Continued.

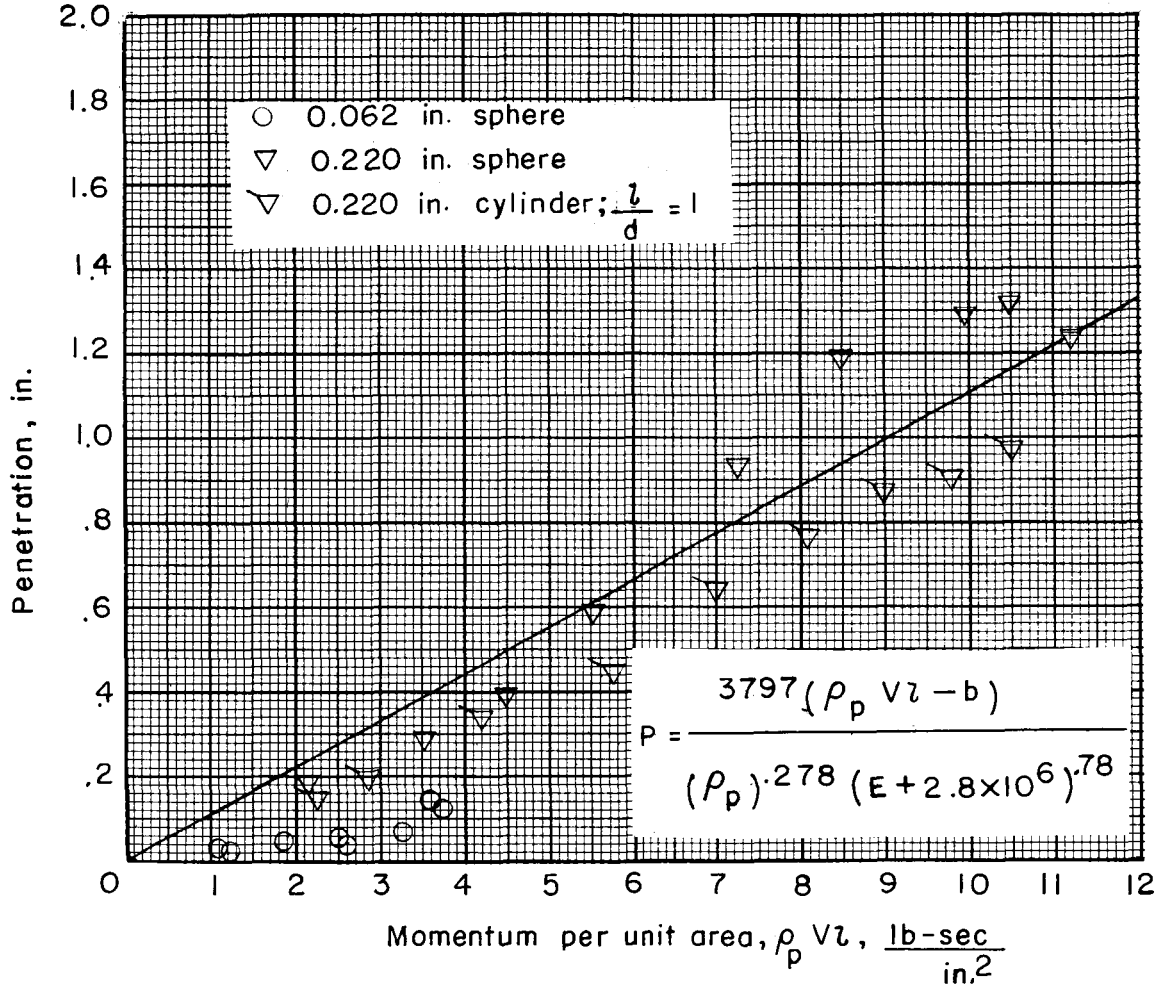

(f) Steel projectiles with impact direction perpendicular to target laminations.

Figure 3.- Concluded.

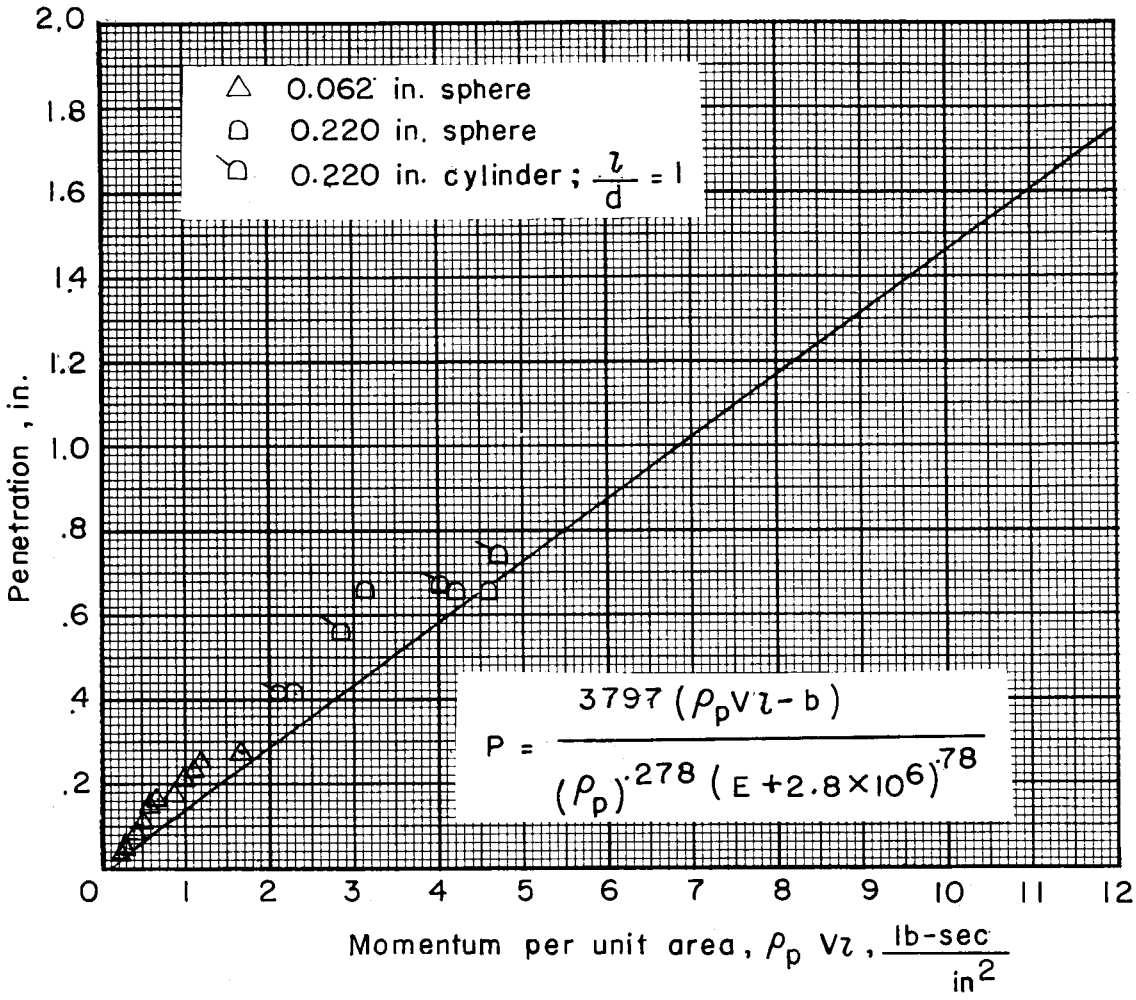

(a) Aluminum projectiles.

Figure 4.- Data of impacts in graphite targets.

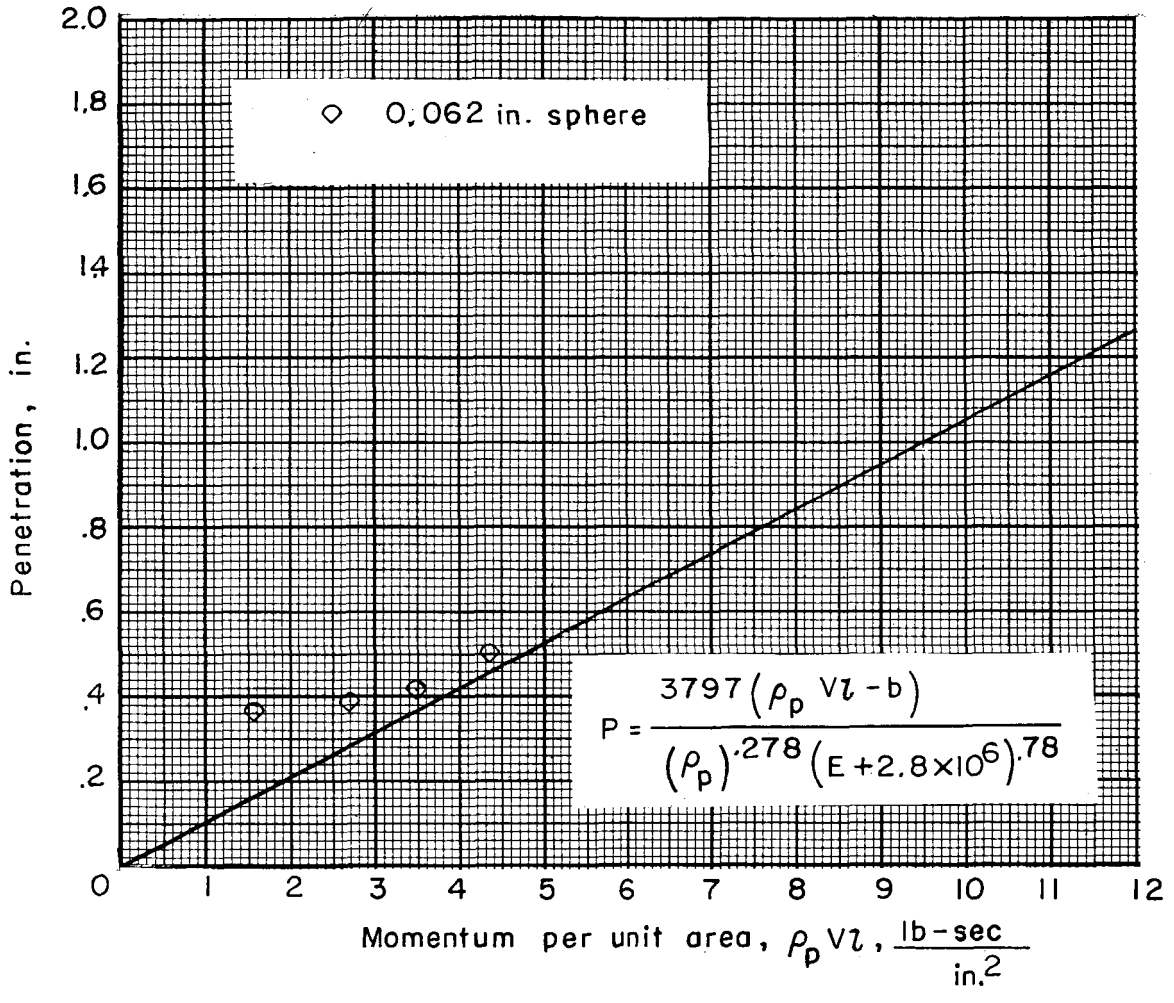

(b) Copper projectiles.

Figure 4.- Continued.

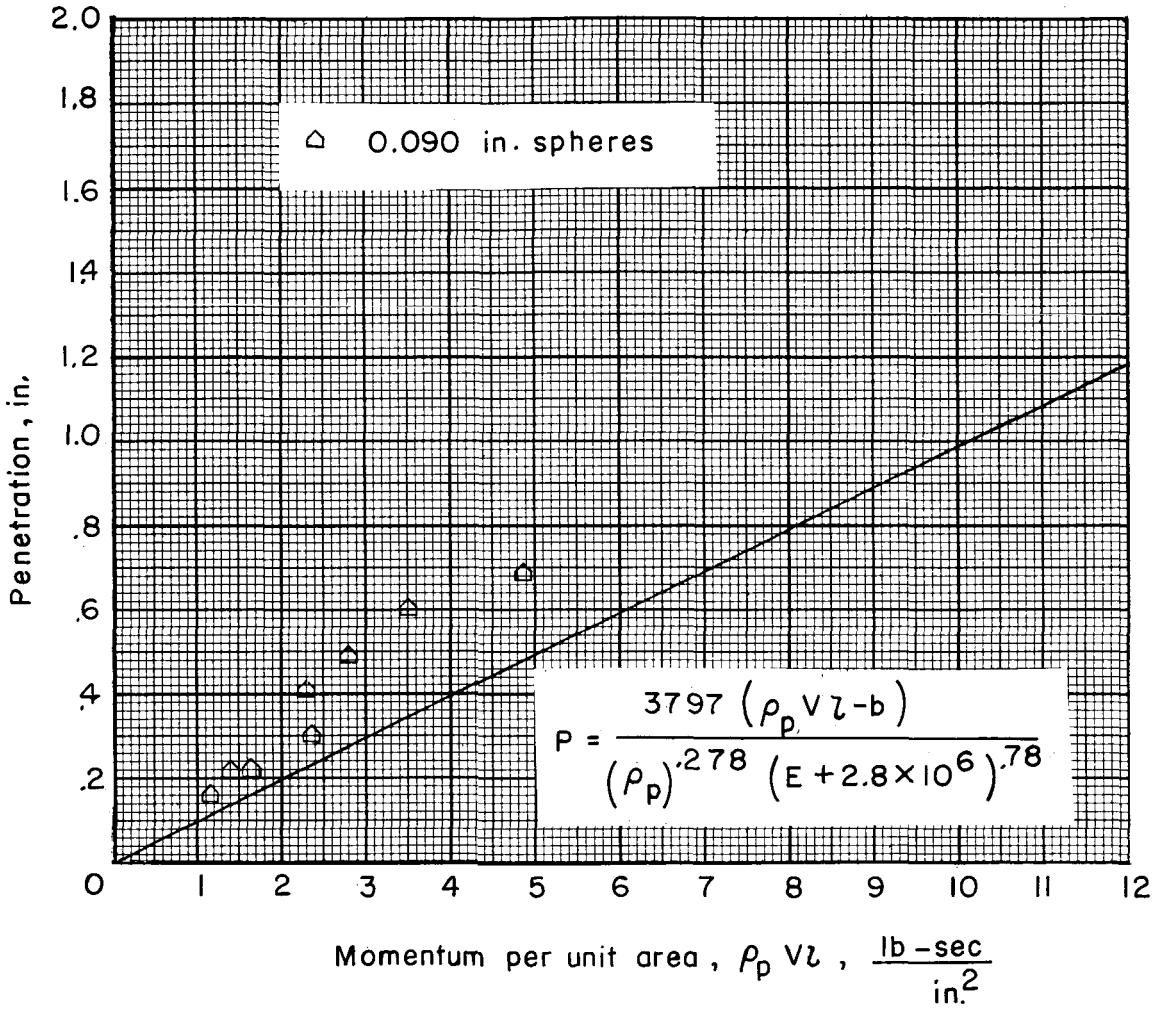

(c) Lead projectiles.

Figure 4.- Continued.

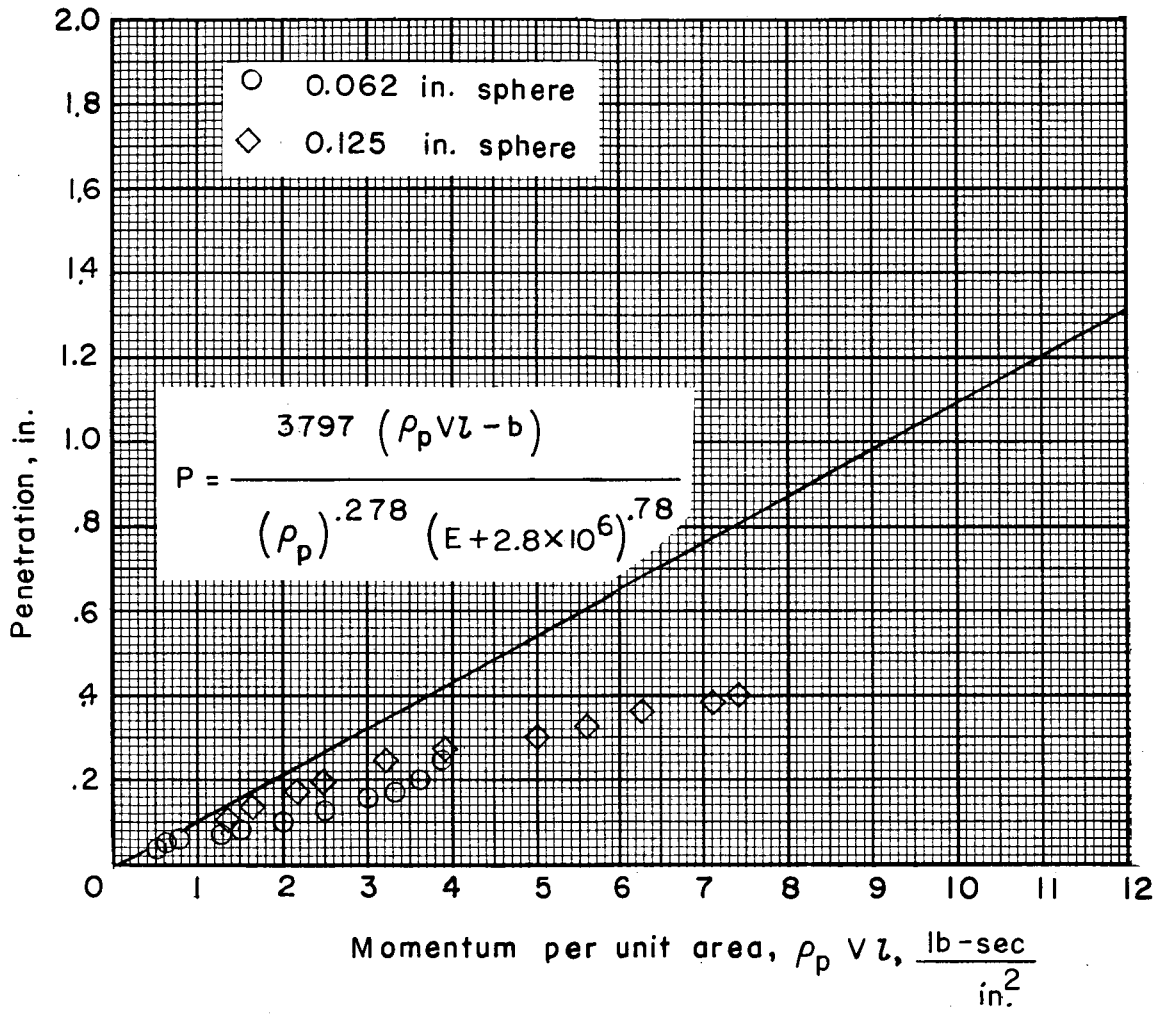

(d) Steel projectiles.

Figure 4.- Concluded.

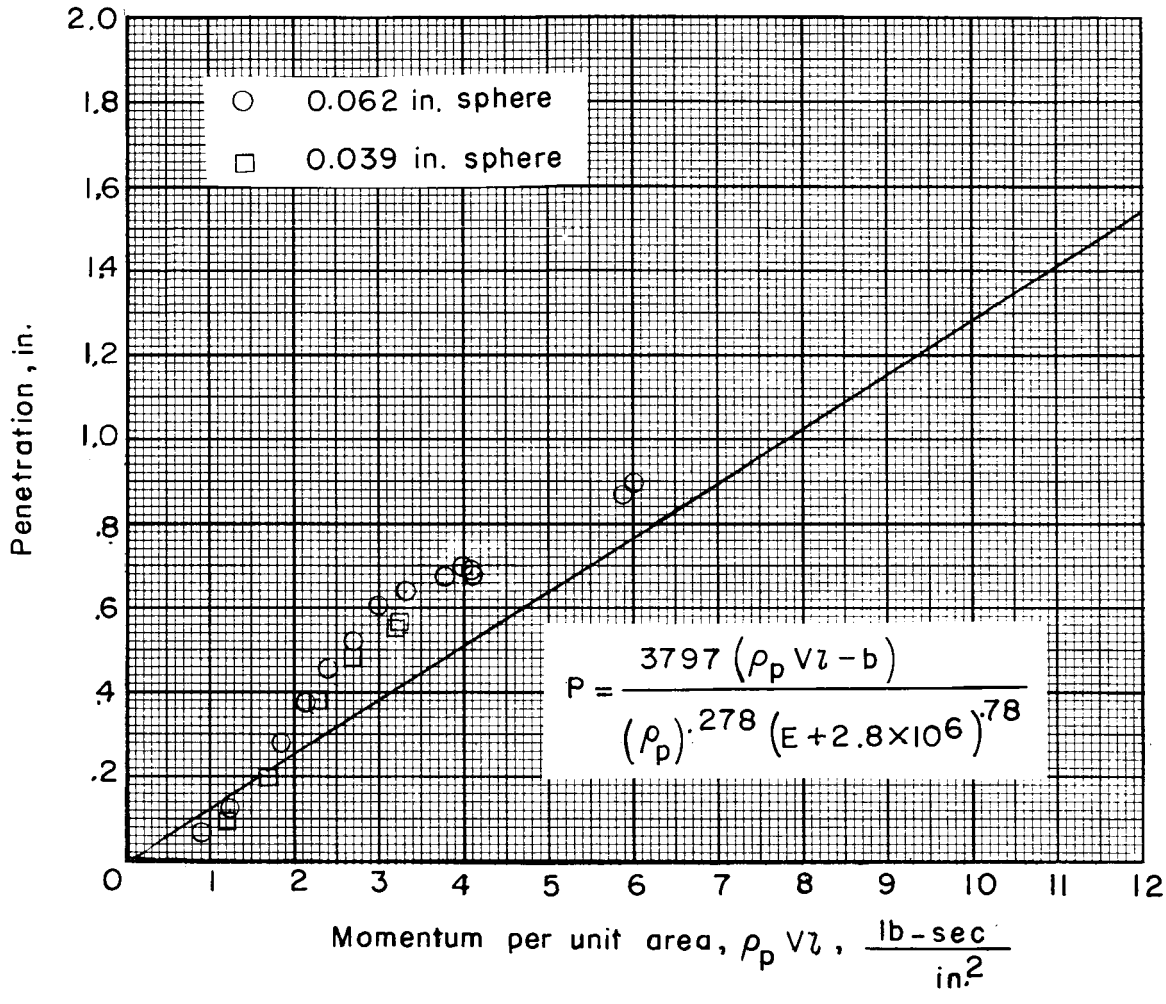

Figure 5.- Data of steel projectiles impacting nylon targets.

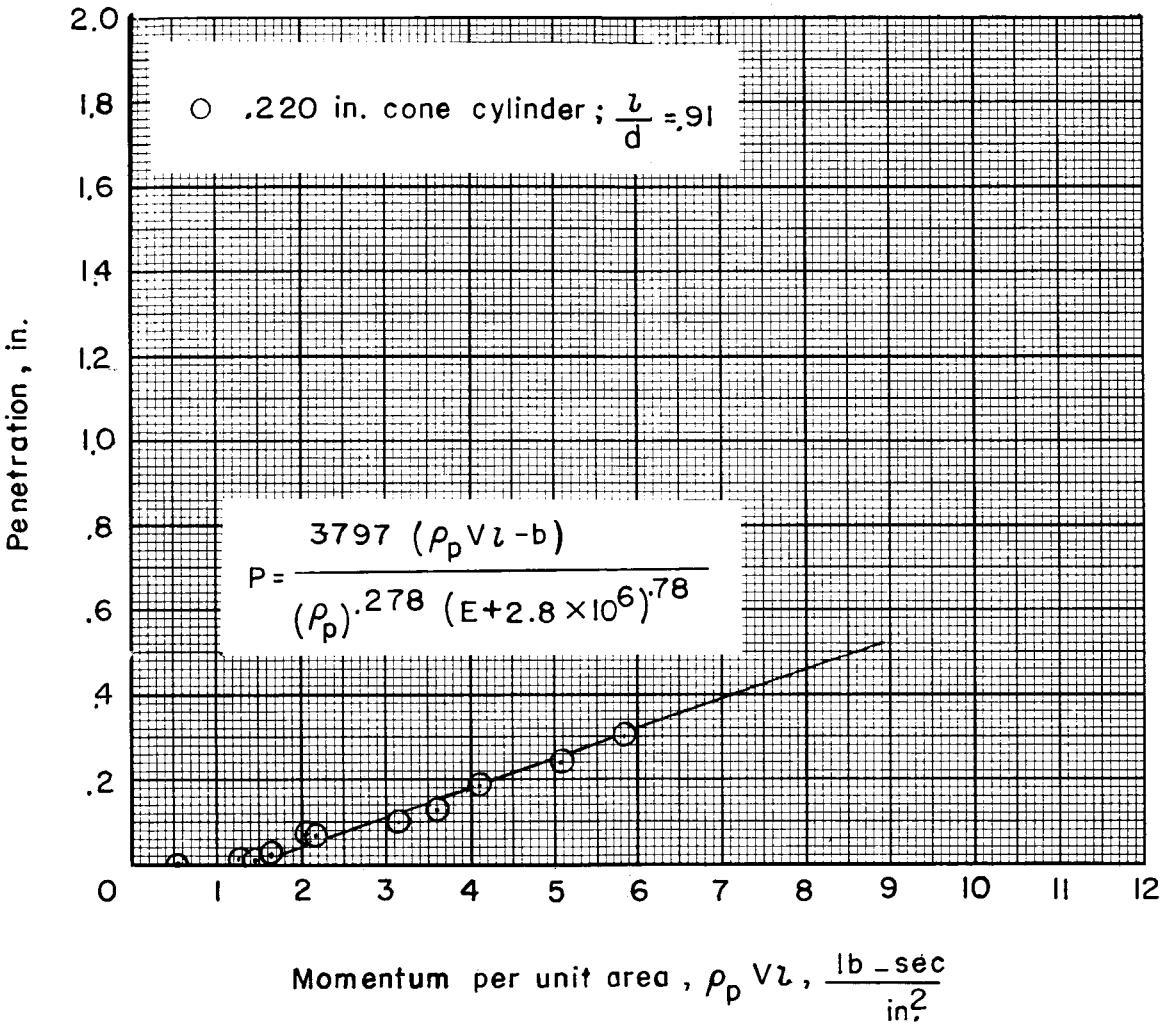

Figure 6.- Data of nylon projectiles impacting aluminum targets.

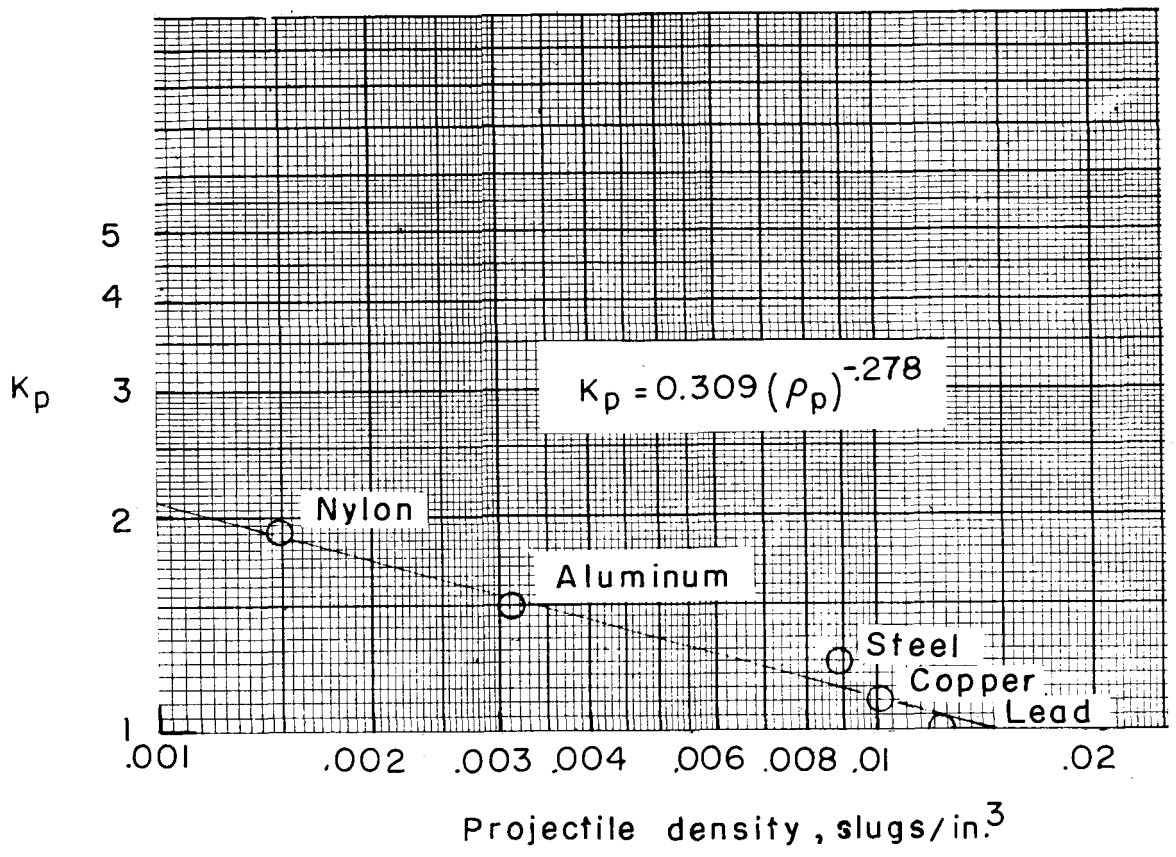

Figure 7.- Experimentally determined values of K_p plotted as function of the projectile density.

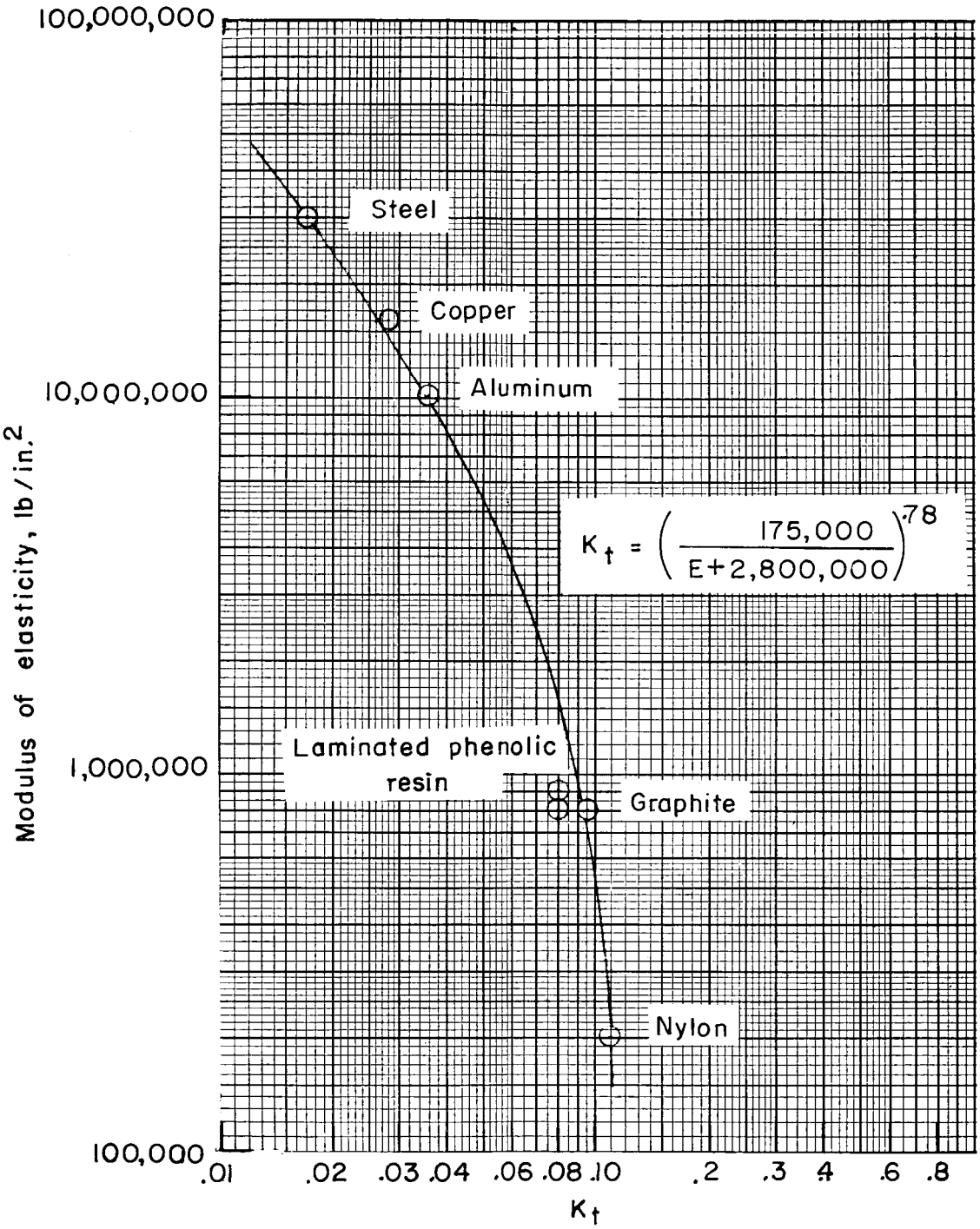

Figure 8.- Experimentally determined values of K_t plotted as function of the target modulus of elasticity.